A Novel Adaptive Cuckoo Search Algorithm for Contrast Enhancement of Satellite Images

Shilpa Suresh, *Student Member, IEEE*, Shyam Lal, *Member, IEEE*, Chintala Sudhakar Reddy, and Mustafa Servet Kiran

***Abstract*—Owing to the increased demand for satellite images for various practical applications, the use of proper enhancement methods are inevitable. Visual enhancement of such images mainly focuses on improving the contrast of the scene procured, conserving its naturalness with minimum image artifacts. Last one decade traced an extensive use of metaheuristic approaches for automatic image enhancement processes. In this paper, a robust and novel adaptive Cuckoo search based Enhancement algorithm is proposed for the enhancement of various satellite images. The proposed algorithm includes a chaotic initialization phase, an adaptive Lévy flight strategy and a mutative randomization phase. Performance evaluation is done by quantitative and qualitative results comparison of the proposed algorithm with other state-of-the-art metaheuristic algorithms. Box-and-whisker plots are also included for evaluating the stability and convergence capability of all the algorithms tested. Test results substantiate the efficiency and robustness of the proposed algorithm in enhancing a wide range of satellite images.**

***Index Terms*—Contrast enhancement, Cuckoo search algorithm, metaheuristics, satellite images.**

I. Introduction

SATELLITE images are widely used in many domains, such as military, astronomy, planning, geoscience studies, and several other humanitarian applications [1], [2]. The visual quality of those remotely sensed images gets degraded owing to the environmental noises and various other interfering factors during their acquisition. Hence, all the image processing and analysis applications necessitates an improvement in the visual attributes of such images.

Image contrast is one among such visual attributes that will significantly contribute to the quality of the image perceived. The variations in the contrast between two adjacent surfaces is produced by the differences in their reflected luminance. Since human visual system is highly sensitive to the image contrast than its absolute luminance, it is perceived as the difference in the color and brightness of those objects. Low-contrast regions appear to be dark and regions with very high contrast appears as artificially illuminated. Both will result in the loss of relevant information. So, the problem is to optimally enhance the image contrast so as to represent all the information present in the input image. Hence, image enhancement is been adopted as an elementary step in all digital image processing and analysis applications to improve the interpretability or information perceived by humans [3], [4].

Histogram equalization (HE) and its variants are the most common and basic methods adopted for image enhancement [5]–[9]. Numerous methods ranging from the simple linear contrast stretch to highly sophisticated adaptive algorithms, in both spatial and transform domains, are available in the literature for image contrast enhancement [10]–[15]. Since most of those enhancement approaches are image-dependent, they cannot be generalized and automated. It also resulted in several image artifacts making the output image harsh and noisy.

The process of automating an image enhancement procedure involves defining an adaptive transformation function applicable for a wide range of image datasets. A robust evaluation criterion can be, hence, adopted to adapt the transformation function to the chosen input image dataset. Metaheuristic optimization algorithms opened a new pace in this contest during the last few decades. The guided random search procedure followed by such algorithms helped in solving even these complex contrast enhancement problems.

A plethora of literature reveals the use of several metaheuristic algorithms towards image enhancement applications in different domains. In 1994, Genetic algorithm (GA) was used by Pal *et al.* for automatic selection of image enhancement operator [16]. Later, in 1999, Saitoh was reported to use GA to model the transformation function for intensity mapping to enhance the contrast of the input image [17]. The method produced reasonably good results in expense of execution time. A similar method was proposed by Munteanu and Lazarescu in the same year, to evolve the contrast stretching curve using real-coded GA and was successfully tested on a dataset comprising remote sensing images [18]. But the use of a highly subjective fitness criterion made it less reliable. In 2000, Munteanu and Rosa put forward a local enhancement technique driven by GA, following

Manuscript received December 9, 2016; revised February 13, 2017 and March 18, 2017; accepted April 16, 2017. Date of publication June 5, 2017; date of current version August 9, 2017. *(Corresponding author: Shyam Lal.)*

S. Suresh and S. Lal are with the Department of Electronics and Communication Engineering, National Institute of Technology Karnataka, Surathkal 575025, India (e-mail: shilparagesh89@gmail.com; shyam.mtec@gmail.com).

C. S. Reddy is with the Forestry & Ecology Group, National Remote Sensing Centre, Indian Space Research Organisation, Hyderabad 500037, India (e-mail: drsudhakarreddy@gmail.com).

M. S. Kiran is with the Department of Computer Engineering, Selcuk University, Konya 42250, Turkey (e-mail: mustafaservetkiran@gmail.com).

This paper has supplementary downloadable material available at http://ieeexplore.ieee.org. The supplementary material includes the quantitative and qualitative experimental results obtained on comparing the seven performance assessment measures for eight different enhancement algorithms discussed in the paper for three more satellite images. The total size of the file is 12.8 MB. Color versions of one or more of the figures in this paper are available online at http://ieeexplore.ieee.org.

Digital Object Identifier 10.1109/JSTARS.2017.2699200

a predefined fitness criterion for image enhancement [19]. The improved efficiency of the proposed technique over point operations like HE and linear contrast stretching (LCS) was achieved compromising the computational complexity factor which required to be answered.

Later, in 2007, Braik *et al.* investigated the use of Particle Swarm Optimization (PSO) algorithm for image enhancement by maximizing the entropy and edge details of the transformed image [20]. Gorai and Ghosh also furnished a similar analytical study based on PSO for parameter optimization for image enhancement in the forthcoming years [21], [22]. Although PSO-based enhancement methods were computational less complex compared with similar methods using GA, they were not tested on color images to substantiate its robustness. Dos Santos Coelho *et al.* [23] proposed three variants of differential evolution (DE) algorithm based on chaotic functions for image enhancement by adopting the same fitness function used by Braik *et al.* [20]. Even though, the use of chaotic sequences ensured the fast convergence of the algorithm, the authors failed to give adequate analytical and statistical proofs highlighting its image enhancement quality.

Nearly all contrast enhancement algorithms, evolve compromising the mean intensity of the image in cost of its subjective efficiency. But it is rational to preserve the mean intensity of an image, since it profoundly contribute in avoiding unwanted artifacts while enhancement. In 2009, Kwok *et al.* devised a Multiobjective particle swarm optimization (MPSO)-based contrast enhancement technique for preserving the mean intensity of the image [24]. Gray scale images with different intensities and distribution were chosen for testing. But test results showed instances of discrepancies to ideal cases by attaining maximum entropy values for zero intensity difference [24]. In 2014, Shanmugavadivu and Balasubramanian formulated a brightness preserving image contrast enhancement method [25]. The proposed technique ensured the avoidance of the abrupt mean shift that used to occur during equalization process. But it suffered from a drawback of being less stable and computationally complex [25]. Later, in 2015, Bhandari *et al.* introduced beta DE algorithm for modeling optimized transformation matrix for intensity mapping [26]. The experimental results furnished were quantitatively better, but it resulted in intensifying the noise present in the image. Further none of the above optimization algorithms were tested for multiband images to evaluate its robustness. Recently, in 2016, researchers have presented a comprehensive analytical evaluation on the use of different contrast enhancement techniques on satellite images [27], [28].

In this paper, a novel adaptive Cuckoo search based enhancement algorithm (ACSEA) is proposed for contrast enhancement of satellite images. The process is automated by optimizing a well-defined enhancement kernel ensuring an optimal contrast stretch for the processed image. The proposed algorithm includes a Chaotic initialization phase, an adaptive $L\acute{e}vy$ flight strategy and a mutative randomization phase. The main contributions of this research paper are summarized as follows.

1) The proposed algorithm adopts a chaotic initialization phase, which helps in effectively avoiding its premature convergence to the suboptimal solutions.
2) The fitness value depended adaptive $L\acute{e}vy$ flight strategy significantly helps in improving the convergence rate of the standard Cuckoo search algorithm.
3) The inclusion of a mutative randomization strategy facilitates an efficient balancing of the exploration and exploitation phases of the proposed algorithm, which ensures the best possible optimum solution for the problem considered.

The novelty of the proposed algorithm accounts for the fact that the impact of these three modifications on standard CS algorithm was not tested for the optimization of any two-dimensional (2-D) signal processing scenarios till date, to the best of our knowledge. This also provides a significant contribution to state-of-the-art optimization-based image enhancement algorithms, particularly in remote sensing domain.

The rest of this paper is structured as follows. Section II gives a detailed discussion about the problem formulation for image enhancement. The structural framework of the proposed image enhancement algorithm is explained in Section III. Section IV includes the simulation results and discussions on comparing the proposed algorithm with various state-of-the-art nature inspired optimization algorithms. Qualitative and quantitative comparisons with some nonnature inspired algorithms, recently employed in remote sensing domain, is included in the supplementary material. Section V concludes the discussion by highlighting the advantages of the proposed algorithm, giving scope for future investigations.

II. Problem Formulation

Image contrast enhancement process can be considered as a nonlinear optimization problem wherein the objective is to enhance the visual contrast of the input image, minimizing unwanted artifacts. Automation of enhancement process involves defining a transformation function, termed as enhancement kernel for mapping the input pixel intensity values to a new set, and a fitness function to quantify the quality of the enhanced image. Detailed discussions on the related functions used for the proposed enhancement process is presented in this section.

A. Enhancement Kernel

Image contrast enhancement in spatial domain is carried out by generating new intensity values for an input image with dimensions "$M \times N$" by altering the spatial relationship between the pixels contained. "M" denotes the number of rows and "N" denotes the number of columns used to represent the image. A transformation function will help in this mapping process which transforms the original image into its contrast enhanced version.

The proposed enhancement algorithm uses a transformation function that includes both global and local attributes of the input image. Hence, we can mathematically formulate the required enhancement process given as

$$O_{(i,j)} = (\mu^L_{(i,j)})^a + \boldsymbol{F^e}_{(i,j)}\left(I_{(i,j)} - c \times \mu^L_{(i,j)}\right)$$
$$\text{where } \boldsymbol{F^e}_{(i,j)} = k\frac{\mu^G}{\sigma^L_{(i,j)} + b}. \tag{1}$$

$\boldsymbol{F^e}_{(i,j)}$ is termed as the image enhancement function, which depends on the global mean and local standard deviation of the input image. The local standard deviation about $(i,j)\text{th}$ pixel of an image is measured by calculating the standard deviation of pixel intensity values over a range specified by a window of size "$n \times n$" centered at (i,j). Similarly, $\mu^L_{(i,j)}$ specifies the local mean of pixel intensities of the input image denoted by (3). Mathematical formulation of global mean, local mean, and local standard deviation of an image is given in (2)–(4), respectively

$$\mu^G_{(i,j)} = \frac{1}{M \times N} \sum_{i=1}^{M} \sum_{j=1}^{N} I_{(i,j)} \tag{2}$$

$$\mu^L_{(i,j)} = \frac{1}{n \times n} \sum_{i=1}^{n} \sum_{j=1}^{n} I_{(i,j)} \tag{3}$$

$$\sigma^L_{(i,j)} = \left(\frac{1}{n \times n} \sum_{i=1}^{n} \sum_{j=1}^{n} \left(I_{(i,j)} - \mu^L_{(i,j)} \right)^2 \right)^{\frac{1}{2}}. \tag{4}$$

We need to optimize the four dependent parameters a, b, c, and k for modeling a robust transformation function. Equation (1) can be, hence, rewritten as (5) to form the required transformation function for the proposed algorithm.

$$O_{(i,j)} = (\mu^L_{(i,j)})^a + k \frac{\left(I_{(i,j)} - c \times \mu^L_{(i,j)} \right) \mu^G}{\sigma^L_{(i,j)} + b}. \tag{5}$$

The transformation function depicted in (5) stretches the image contrast centered at its local mean. $(a,b,c,k) \in \mathbb{R}^+$ are the four related parameters of the enhancement kernel. The base method for this transformation kernel detailed by Gonzalez, allows a very restricted selection of values for "b" and "c" [7]. The parameter "b" was fixed at a value "0" making the denominator of the enhancement kernel to depend only upon the local standard deviation of the image. Thus, a zero local standard deviation across the selected window makes the kernel unstable. Whereas, the proposed algorithm allows the parameter "b" to range between $(0, 0.5)$, which makes the technique more feasible by allowing a chance for having a zero standard deviation along the chosen window. Similarly, the parameter "c" was fixed to a value "1" in the older method, which was then modified to take up fractional values to allow the subtraction of a fraction of the local mean value from the original image intensity value. Likewise, the insertion of the first term in (5) was another modification to the fundamental method which regulates the smoothening and brightening effect on the processed image [28]. Thus, the new selection for the parameters (a,b,c,k) allows the broadening of the transformation spectrum. Since these parameters regulate the amount of stretch, capable of bringing variations in the intensity values of processed image, the proposed enhancement algorithm is designed to optimize these set of parameters.

B. Evaluation Criterion

A fitness function can be summarized as a figure of merit to evaluate how close a designed solution is in achieving the desired aims. In particular, the convergence of any optimization algorithm is attained by testing a fitness function in each iteration till the result satisfies the desired quality. Apart from attaining close correlation to the designer's goal, a fitness function also regulate the execution speed of an optimization algorithm. Thus, a good fitness function should contain all significant testing parameters, which can be quickly computed for quantifying the quality of the current input solutions set. Literature reveals the use of different such evaluation conditions for judging the enhancement quality of a processed image [21], [29], [30].

The proposed algorithm for image enhancement adopts a fitness criterion as a function of the edge information, including the number of relevant edges as well as its intensity values, and the entropy of the processed image. A contrast enhanced image is observed to have more number of relevant edges with higher intensity levels as compared with the original input image. A good contrast enhanced image stretches the contrast by redistributing the intensity values, meanwhile equalizing the resultant histogram increasing the entropy of the image. An increased entropy value will directly quantify an increase in the information content of the image, which can be used as a measurable entity to access the quality of enhancement. The inclusion of entropy value of the processed image also helps to reduce the noise intensification effects which may result in artificial binary images with very low intensity span. An increased entropy value also ensures a wider pixel intensity range in the processed image, which contributes in preserving the naturalness of the captured scene.

Since an increase in the entropy value of the processed image do not specify the existence of relevant edges, a local operant which can gauge the edge information is inevitable in devising a fitness criterion for evaluating the contrast enhancement of an image. A simple edge detection approach using Sobel edge detector can, hence, be included in the fitness function. Compared with Canny and Laplacian edge detection operators, Sobel operator is regarded to be highly reliable and, hence, a good choice for distinguishing and quantifying the edge information content in the processed image [7], [31], [32].

Although the use of Sobel edge detector helps in finding the relevant edge details, it fails in ensuring a good contrast in other regions of the image. Hence, a combination of these two operands can be a good choice for designing a fitness function for a better image enhancement algorithm.

The fitness function evaluated in the proposed enhancement algorithm is given by the equation

$$F(O) = \log\Big(\log\big(E(O^s) + \boldsymbol{e}\big)\Big) \cdot \frac{N_e(O^s)}{M \times N} \cdot e^{H(O)} \tag{6}$$

where $O^s_{(i,j)} = \sqrt{(\nabla_x O_{(i,j)})^2 + (\nabla_y O_{(i,j)})^2}$; $\nabla_x O_{(i,j)} = (g_{(i-1,j+1)} + 2g_{(i,j+1)} + g_{(i+1,j+1)}) - (g_{(i-1,j-1)} + 2g_{(i,j-1)} + g_{(i+1,j-1)})$; $\nabla_y O_{(i,j)} = (g_{(i+1,j+1)} + 2g_{(i+1,j)} + g_{(i+1,j-1)}) - (g_{(i-1,j+1)} + 2g_{(i-1,j)} + g_{(i-1,j-1)})$.

The term $g_{(i,j)}$ denotes the gray level intensity value of the enhanced image O specified by the coordinate values (i,j), $E(O^s)$ is the sum of all the pixel intensity values of Sobel edge

detected image O^s given as

$$E(O^s) = \sum_{i=1}^{M} \sum_{j=1}^{N} O^s_{(i,j).} \tag{7}$$

$N_e(O^s)$ in (6) denotes the total number of edge intensities in the sobel edge detected image whose value is greater than a defined threshold. The threshold value is automatically generated depending on the signal to noise ratio of the image [33].

$H(O)$ gives the entropy of the processed image, which directly reflects the information content present in the image. Hence, a wider range of intensity values (high contrast) yield a higher entropy value. It can, thus, be used as a measure to access broadening of the spectrum which indirectly performs a HE. The entropy of enhanced image $H(O)$ is given as [34]

$$H(O) = -\sum_{i=0}^{L_{\max}-1} p(i)\log_2(p(i)) \tag{8}$$

where $p(i)$ indicates the probability of occurrence of pixels with intensity value $i \in (0, L_{\max} - 1)$ in the enhanced image (O) and $L_{\max}$ denotes the maximum intensity value present in the enhanced image.

Empirical evidences proved that the factor $E(O^s)$ varies within three orders of magnitude where as $H(O)$ varies within one order of magnitude lesser than the other components in the fitness function. A log-log measure of $E(O^s)$ in (6) is, thus, chosen to limit the over emphasis of term in the fitness function, which may produce unnatural images with very high contrast. The parameter "e" in (6) is the Euler constant, which is used to avoid undefined points when the edge intensity is "0." Similarly the effect of the slowly varying term $H(O)$ in the fitness function is balanced by taking its exponential value [35]. Therefore, a maximization of the defined fitness function, in turn maximizes the number of significant edges, with higher intensities (sharp edges) and the entropy of the processed image.

III. Proposed Novel Adaptive Cuckoo Search based Enhancement Algorithm

The objective of designing proposed optimization algorithm is to solve for the optimum quartet (a, b, c, k) that will help in effectively enhancing the input image. Each of those parameters are bound to some boundary constraints given by $a \in [0, 1.5]$, $b \in [0, 0.5]$, $c \in [0, 1]$, $k \in [0.5, 1.5]$. x_i corresponds the ith candidate vector in the population which denotes a parameter quartet computed using (9) with $x^{\min} = [0, 0, 0, 0.5]$, $x^{\max} = [1.5, 0.5, 1, 1.5]$.

The proposed algorithm is a modified version of Cuckoo search (CS) algorithm, developed by Yang *et al.* [36]. The selection of CS algorithm, being one among the recent metaheuristic optimization algorithms, was based on a prior empirical study, highlighting its improved performance in solving various nonlinear optimization problems [37], [38]. The main advantages of CS algorithm over others are: 1) its simplicity in implementation, since it depends only on a single control parameter apart from the population size; 2) the use of *Lévy* flight instead of Brownian random walks aims to speed up the convergence, owing to the fast increase in its variance compared with the other. These features also make it easily adaptable with multicriteria optimization problems and can be even hybridized with other swarm-based algorithms.

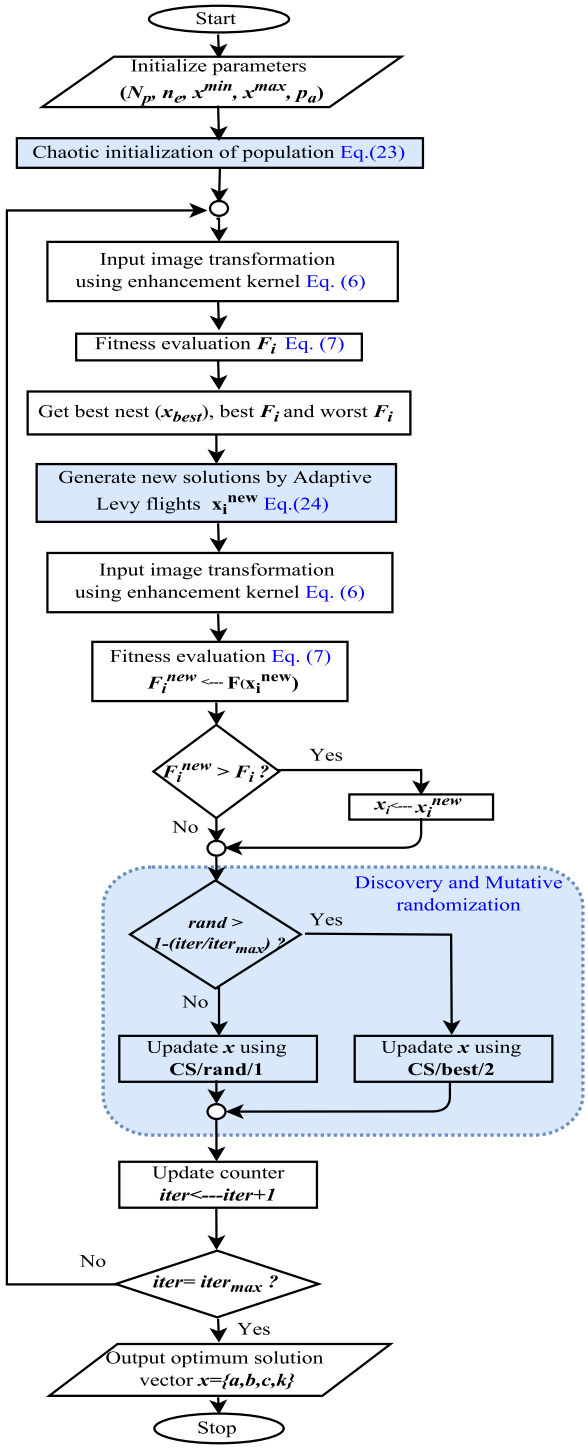

Fig. 1. Flowchart of proposed ACSEA.

The three major modifications to the standard CS algorithm includes a chaotic initialization phase, an adaptive *Lévy* flight strategy and a mutative randomization phase which are described below. Fig. 1 depicts the flowchart of the proposed algorithm.

A. Chaotic Initialization

One among the major alterations in the standard CS algorithm is the inclusion of a chaotic function based initial population generation, which will helps in the making the algorithm to converge fast. A logistic chaotic function mathematically defined as in (9) is adopted for initializing the solution space [39], [40]

$$x_{i,j}(t) = x_j^{\min}(t) + (x_j^{\max}(t) - x_j^{\min}(t)) \cdot ch_t(n_e)$$
$$\text{where } ch_{t+1} = \boldsymbol{K} \cdot ch_t(1 - ch_t) \tag{9}$$

where $i = 1, 2, ...N_n$; $j = 1, 2, 3, 4$ ($n_e = 4$ for our case). The chaotic parameter $ch_t \in (0, 1)$; $t = 0, 1, 2, ...T$, $ch_0 \notin \{0.0, 0.25, 0.75, 0.5, 1.0\}$; $0 < \boldsymbol{K} \leq 4$. The maximum number of chaotic iterations is denoted by T and $\boldsymbol{K}$ is the control parameter which determines the behavioral characteristics of the mapping function [23]. Hence, for our case $x_i(t) = [x_{i,1}(t), x_{i,2}(t), x_{i,3}(t), x_{i,4}(t)]$ where $x_{i,1}(t) = a$, $x_{i,2}(t) = b$, $x_{i,3}(t) = c$, $x_{i,4}(t) = k$, $x^{\min} = [a_l, b_l, c_l, k_l], x^{\max} = [a_h, b_h, c_h, k_h]$.

Initialization phase also includes manual assignment of values used by different parameters along the run of the proposed algorithm. It includes the total number of nests (N_n), number of eggs in each nest (n_e), switching (alien egg discovery) parameter ($p_a \in [0, 1]$), boundary constraints for $(a, b, c, k), i.e\,\{[a_l, a_h], [b_l, b_h], [c_l, c_h], [k_l, k_h]\}$

B. Fitness Evaluation

The fitness function defined in Section II-B is used to evaluate the best solution so far, by computing the fitness of each individual $x_i(t)$. It includes a prior transformation phase of the input image I using the defined transformation function as given in (5) using all the possible solution vectors initialized previously. Those transformed images "O" are used to evaluate the fitness of the solution set using (6).

C. Adaptive Lévy Flights Generation

Lévy flights are random walks with step length drawn from the *Lévy* distribution, according a simple power-law formula given as

$$L(s) \sim \mid s \mid^{-1-\beta} \quad 0 < \beta \leq 2. \tag{10}$$

Generalized Levy distribution can be mathematically represented as

$$L(s, \gamma, s_\mu) = \begin{cases} \sqrt{\frac{\gamma}{2\pi}} e^{\left(-\frac{\gamma}{2(s-s_\mu)}\right)} \frac{1}{(s-s_\mu)^{1.5}}, & 0 < \mu < s < \infty \\ 0, & \text{elsewhere} \end{cases} \tag{11}$$

where s denotes the step size, s_μ indicates the minimum possible step size and γ is the scaling parameter [41].

The second modification is done in this *Lévy* flight generation phase. The original CS algorithm does not have any control over the step size in its iterative process of reaching the global optima [36]. The scaling factor α is fixed in the original CS algorithm, whereas we modify it by adapting it according to the fitness values generated in its previous iteration. This will again help in speeding up the *Lévy* flight movement, thereby making the algorithm to converge to the optimal solutions rapidly. The adaptive *Lévy* flight is, thus, modeled as

$$x_i(t+1) = x_i(t) + \alpha_i(t+1) \cdot Lévy(s, \beta)$$
$$\text{where } Lévy(s, \beta) = \frac{\beta\Gamma(\beta)\sin(\frac{\pi\beta}{2})}{\pi} \cdot \frac{1}{s^{1+\beta}}, (s \gg 0, \beta = 1.5)$$
$$\alpha_i(t+1) = \frac{1}{t}\left|\frac{\text{bestfit}(t) - \text{fit}_i(t)}{\text{bestfit}(t) - \text{worstfit}(t)}\right| \tag{12}$$

where t represents the current iteration of CS algorithm, $\text{fit}_i(t)$ is the fitness value of ith nest in tth iteration, best fit(t) is the best fitness value and worst fit(t) is the worst fitness value in tth iteration.

It is evident that the step size is initially high, which decreases as the iterations increases. Hence, the step size will be very small when it approaches the global optimal solution. Therefore, (12) clearly indicates that the step size is adaptively decided from the fitness value [42].

D. Discovery and Mutative Randomization

DE is a powerful evolutionary algorithm originally introduced for continuous optimization scenarios, which was later on applied in different domains. It followed a general evolutionary procedure, which included a mutation, cross over, and a selection stage. Different variants of DE were developed following different mutation strategies, which were used successfully in various public domains [41]. DE variants are generalized by denoting them as DE/*x*/*y*/*z*, where *x* is the vector to be mutated, *y* is the number of different vectors considered for mutation, and *z* denotes the crossover scheme employed.

The mutation strategies used by two commonly used variants are given in (13), which are modified and adopted in ACSEA algorithm for implementing a discovery and mutative randomization phase as depicted in the equation [43]

$$\text{DE/rand/1/bin} : z_i(t+1) = x_{r_1}(t) + F \cdot \left(x_{r_1}(t) - x_{r_3}(t)\right)$$
$$\text{DE/best/1/bin} : z_i(t+1) = x_{\text{best}}(t) + F \cdot \left(x_{r_1}(t) - x_{r_2}(t) + x_{r_3}(t) - x_{r_4}(t)\right) \tag{13}$$

where $i \in \{1, \ldots, N_n\}$, r_1, r_2, r_3, and r_4 are random integer indices selected from $i = \{1, ..., N_n\}$, x_{best} is the vector to be perturbed and F the scaling factor. $F \in [0, 1]$ controls the effect of the difference vector in mutation operation which will help in avoiding search stagnation

$$\text{CS/rand/1/bin} : x_i(t+1) = x_{r_1}(t) + p_a \cdot \left(x_{r_1}(t) - x_{r_3}(t)\right)$$
$$\text{CS/best/1/bin} : x_i(t+1) = x_{\text{best}}(t) + p_a \cdot \left(x_{r_1}(t) - x_{r_2}(t) + x_{r_3}(t) - x_{r_4}(t)\right) \tag{14}$$

where p_a is the alien egg discovery rate in CS algorithm. The pseudocode of this phase is as given as

If `rand` $\geq$ 1-$\frac{t}{t_{max}}$ **then**
  CS/best/1/bin ;
else
  CS/rand/1/bin ;
end

where rand $\in (0, 1)$ follows a uniform probability distribution, t denotes the current generation (iteration) index and $t_{\max}$ gives the maximum number of iterations. The randomization of the solution set based on the probabilistic discovery method of CS algorithm is, thus, modified, wherein, it can adopt any one of the two strategies for mutating the individuals. Thus, if random real number generated is greater than $(1 - \frac{t}{t_{\max}})$, then the CS/best/2 is chosen. Or else it will select CS/rand/1 mutation strategy.

It is evident that the probability of selecting one of the two new search strategies is a function of the iteration index. The value of $(1 - \frac{t}{t_{\max}})$ reduces from 1 to 0 as it proceeds through the generations. The process directs the search in such a way that it balances the exploration and exploitation phases of the search algorithm. Initially $(1 - \frac{t}{t_{\max}})$ will be closer to 1, which makes the probability of selecting CS/rand/1 strategy higher compared with CS/best/2. This process, in turn results in extensive exploration. As the iteration increases, we reach a stage where the two new search methods may be used with the same probability. Towards the end of the algorithm, these two search strategies are used in the reverse manner. That is, the probability of choosing the CS/best/2 strategy will be higher compared with CS/rand/1. This results in enhancing the exploitation capability of the algorithm. Hence, based on two new search strategies controlled by a linear decreasing probability rule, the algorithm balances its exploitation and exploration phases [43].

E. Termination Condition

The fitness of the new solution set is evaluated, followed by the previous exploitation and exploration stages till the stopping criterion is met. Finally, the execution of the algorithm ends by generating the best solution vector (a, b, c, k) that optimizes the required scenario.

IV. Results and Discussion

A. Experimental Settings

The performance of the proposed ACSEA was assessed by comparing it with several other nature-inspired heuristic algorithms like *A1*: Particle swarm optimization (PSO) [44], *A2*: Differential evolution (DE) [45], *A3*: Firefly algorithm (FA) [46], *A4*: Cuckoo search (CS) [36], and *A5*: Wind driven optimization (WDO) [47], [48] for solving satellite image enhancement problem. Moreover, two recent metaheuristic algorithms such as *A6*: Beta differential evolution (BDE) [26] and *A7*: Differential evolution-simulated annealing (DESA) algorithm [49] were also considered for comparison.

The selection of these algorithms for results comparison were based on a prior literature study on the optimization algorithms used specifically for image processing applications. We have restricted our study to nature inspired algorithms in order to ensure a fair comparison. The above mentioned algorithms were found to be most common and widely used among them, for various nonlinear image processing applications. All these algorithms have shown a competitive performance when solving complex optimization problems. Hence, a comparison of the proposed algorithm with those will provide a comprehensive assessment on its performance. For further analysis studies have been conducted comparing the proposed algorithm (ACSEA) with four recent nonnature inspired enhancement algorithms used in remote sensing domain. Tables S.IV– S.VIII and Figs. S.7–S.11 in the supplementary material presents the experimental results obtained. The algorithms compared include brightness preserving dynamic histogram equalization [10], [50], singular value equalization [10], [51], discrete wavelet transform and singular value decomposition (DWT-SVD) [10] and regularized-HE and DCT (RHE-DCT) [14].

TABLE I
Parameters Used in Each Algorithm

Algorithm	Parameters	Value
PSO [44]	Inertial factor range $(\omega_{\min}, \omega_{\max})$	(0.4, 0.9)
	Cognitive constant (c_1)	3
	Social constant (c_2)	2
DE [45]	Scaling Factor (F)	0.5
	Cross Over Probability (C_r)	0.2
FA [46]	Attractiveness factor (β)	0.2
	Characteristic length (Γ)	1
	Randomization parameter (α)	0.5
CS [36]	Alien discovery rate (p_a)	0.25
WDO [47]	RT coefficient	2
	Gravitational constant (g)	0.2
	Constant in the update equation (α)	0.5
	Coriolis effect (c)	0.4
	Maximum allowed speed $(P_{\max})$	0.3
BDE [26]	Initial Weighting Factor (F)	0.5
	Crossover rate (CR)	(0, 1)
DE-SA [49]	Scaling factor (F)	0.8
	Crossover constant (C_r)	0.2
ACSEA	Chaotic initialization (ch_0, θ)	(0.75, 2.0)
	Alien discovery rate (p_a)	0.25

The parameter settings of the nature inspired algorithms being compared were adopted from [21], [23], [26], [49] [52]–[54], respectively, which are then properly tuned to suit the problem to be solved. Lower and upper bounds for the four parameters (a, b, c, k) to be optimized were set to be a$\in$ [0, 2], b $\in$ [0,1], c$\in$ [0, 0.5], k$\in$ [0, 2] for all the algorithms compared. The initial population size was set to be 50 and the total number of iterations were fixed to be 100 for all the investigated algorithms. Table I summarizes other parameter settings for each of them. Parameters of the proposed algorithm were set according to the other compared algorithms, so as to allow a fair comparison.

The proposed algorithm was tested on several satellite images procured from NASA, Satpalda geospatial services, and Satellite Imaging Corporation. The images chosen followed different illumination conditions and shown significant contrast disparities throughout the global space, which will clearly demonstrate the usefulness of the proposed algorithm. The experimental results furnished in this paper includes two among them. Similar qualitative and quantitative experimental results of three more images are given in Tables S.I–S.III and Figs. S.4–S.6 in the supplementary material. The algorithms were coded using MATLAB R2015a running on an Intel Core i7 PC with 3.40 GHz CPU and 8 GB RAM.

B. Performance Measures

For evaluating the performance of the proposed algorithm and other state-of-the-art meteheuristic algorithms compared, the following significant fidelity metrics are considered. Image distortion and sharpness of the resultant image are the two important characteristics assessed to judge the efficiency of an enhancement algorithms. Mean Square Error (MSE) is a very frequently used distortion (error) measurement parameter, which need to be minimum for a better enhancement approach. Likewise, PSNR quantify the quality of an image that takes a higher value for an image with less noise content. Thus, it eventually evaluates the similarity measure between the original and processed image based on the MSE values computed over every pixel which is depicted as

$$\text{PSNR(dB)} = 10\log_{10}\left(\frac{\left(L_{\max}-1\right)^2}{\text{MSE}}\right)$$

$$\text{where MSE} = \frac{1}{MN}\sum_{i=1}^{M}\sum_{j=1}^{N}\left[I_{(i,j)} - O_{(i,j)}\right]^2 \tag{15}$$

where "M" and "N" denote the dimensionality of the image and "I" & "O" refers to the input and output processed images, respectively, [37].

Another important metric value used to evaluate the contrast enhancement of a coloured image is $color\ enhancement\ factor$ (CEF) [55]. The mathematical formulation of the CEF metric is given as

$$\text{CEF} = \frac{\text{CM}(O)}{\text{CM}(I)} = \frac{\sqrt{\sigma_{\alpha_O}^2 + \sigma_{\beta_O}^2} + 0.3\sqrt{\mu_{\alpha_O}^2 + \mu_{\beta_O}^2}}{\sqrt{\sigma_{\alpha_I}^2 + \sigma_{\beta_I}^2} + 0.3\sqrt{\mu_{\alpha_I}^2 + \mu_{\beta_I}^2}} \tag{16}$$

where $\alpha = R - G$ and $\beta = \frac{R+G}{2} - B$, σ and μ represent the standard deviation and mean of respective values α and β. Subscripts "I" and "O" with each parameter specifies whether the measured parameter is for the original or enhanced image [55], [56].

Structure similarity index (SSIM) gives the measure of edge information content in the processed image. It is measured by evaluating the similarity in the high frequency content (edge information) of processed (enhanced) and original image [57]. A higher value of SSIM indicates a better performance of the enhancement algorithm. It is mathematically represented given as [57]

$$\text{SSIM}(I, I^t) = \frac{(2\mu_I\mu_O + \psi_1)(2\sigma_{IO} + \psi_2)}{(\mu_I^2 + \mu_O^2 + \psi_1)(\sigma_I^2 + \sigma_O^2 + \psi_2)} \tag{17}$$

where (μ_I, μ_O), (σ_I, σ_O), and (σ_I^2, σ_O^2) represent the mean, standard deviation, and variance of the input and output image, respectively, σ_{IO} denotes the covariance between input and output images and $(\psi_1\ ,\ \psi_2)$ are two constants.

Universal quality index (UQI) proposed by Wang *et al.* in 2002 is a quality measure applicable universally for all image processing problems [58]. For UQI assessment an image is considered as a combination of loss of correlation, luminance distortion, and contrast distortion factors.

UQI is mathematically evaluated as

$$\text{UQI} = \frac{\sigma_{xy}}{\sigma_x\sigma_y}\cdot\frac{2\bar{x}\bar{y}}{(\bar{x})^2 + (\bar{y})^2}\cdot\frac{2\sigma_x\sigma_y}{\sigma_x^2 + \sigma_y^2}$$

$$\text{UQI} = \frac{4\sigma_{xy}\bar{x}\bar{y}}{\left(\sigma_x^2 + \sigma_y^2\right)\left[(\bar{x})^2 + (\bar{y})^2\right]} \tag{18}$$

where $(\bar{x}, \bar{y})$, (σ_x, σ_y), and σ_{xy} denote the sample means, standard deviations, and covariance between the input and output 1-D vectors, $\mathbf{x} = \{x_i \mid i = 1, 2, ..N\}$ and $\mathbf{y} = \{y_i \mid i = 1, 2, ...N\}$, respectively. For 2-D images overall UQI is evaluated by combining the local UQI values calculated for the entire span of the image using sliding window technique given as

$$\text{UQI}^{\text{overall}} = \frac{1}{B}\sum_{j=1}^{B}\text{UQI}^{\text{local}} \tag{19}$$

where $\text{UQI}^{\text{local}}$ is the local UQI measure, B is the total number of windows (steps) considered.

Structural contrast-quality index (SC-QI) is a recent full reference image quality assessment method devised by Bae *et al.*, [59], which can well characterize local and global visual quality perceptions. The detail analysis of the steps included in computing SC-QI score is given in [59]. The overall SC-QI score of an image can be, thus, calculated by

$$\text{SC-QI}_{(I,O)} = \frac{1}{W}\sum_{m=1}^{B} w\ \left(x^{(m)}, y^{(m)}\right)\ f\ \left(x^{(m)}, y^{(m)}\right) \tag{20}$$

where $w(x, y)$ is the local weight based on visual priors with respect to its local importance (e.g., degree of image content information, phase congruency, visual saliency index, etc) and W is a normalization factor which is calculated as the summation of all $w(x, y)$ values over all B local image blocks.

SC-DM index is an extended version of SC-QI, which includes a distortion assessment measure of the form as given in (21), a local SC-DM measure as given in (22), and two different feature descriptors [60]

$$d(\phi_x, \phi_y \mid \theta) := \text{NRMSE}(\phi_x, \phi_y \mid \theta) = \frac{\mid \phi_x - \phi_y \mid}{\sqrt{\phi_x^2 + \phi_y^2 + \theta}} \tag{21}$$

$$f(x, y) = \parallel d \parallel_2^2 \tag{22}$$

C. Illustration of Proposed ACSEA

The proposed ACSEA includes three modifications to the standard CS algorithm. A chaotic initialization phase was adopted to improve the convergence rate. The intrinsic stochastic property and ergodic nature exhibited by chaotic systems eventually helps the algorithm to reach its global optimum [39]. The second modification includes the use of an adaptive $Lévy$ flight strategy depended on the previous fitness solutions of the problem of interest, which will indeed help in increasing the convergence rate by initiating efficient exploitation around the highly probable solution space. The third modification,

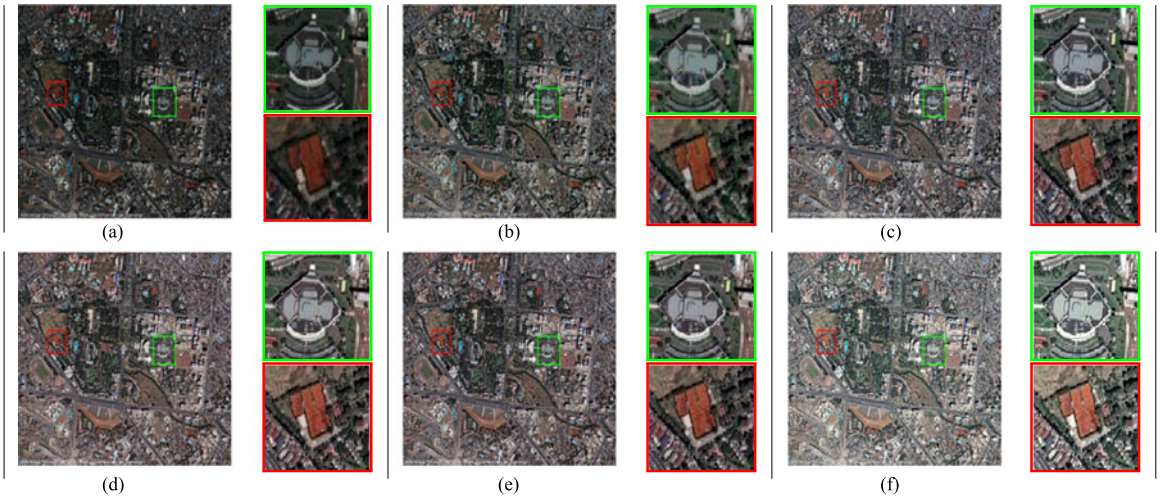

Fig. 2. Enhancement results of Image 2: Addis Ababa, Ethiopia (a) Original; (b) CS; (c) M1; (d) M2; (e) M3; (f) ACSEA.

TABLE II
PERFORMANCE METRICS COMPARISON OF DIFFERENT MODIFIED VERSIONS OF CS ALGORITHM

Algorithm	PSNR	MSE	SSIM	CEF	UQI	SC-QI	SC-DM
CS	23.3628	299.7767	0.8671	0.9892	0.9982	0.9997	0.00030
M1	23.5582	286.5894	0.8873	1.3729	0.9983	0.9998	0.00030
M2	23.4731	292.2632	0.8828	1.3277	0.9982	0.9998	0.00025
M3	23.5683	285.9201	0.8823	1.3834	0.9982	0.9998	0.00024
ACSEA	**23.6427**	**281.0697**	**0.8983**	**1.9291**	**0.9983**	**0.9998**	**0.00020**

i.e., the mutative randomization phase, helps in keeping proper balance between the exploration and exploitation stages of the algorithm.

The effect of each modification on the standard CS algorithm (*M1*: CS algorithm with chaotic initialization, *M2*: CS algorithm with adaptive Levy flight strategy, *M3*: CS algorithm with mutative randomization) are investigated in this section and the results are presented in Fig. 2 and Table II. The convergence plots using the above five CS variants for the same image is given in Fig. 3, which clearly substantiate the effect of each modification on the standard CS algorithm.

On analyzing the plots, the use of chaotic initialization phase have resulted *M1* to reach a near approximation of the attainable global solution without bringing any significant improvement to the convergence rate compared with CS. The use of adaptive *Lévy* flights in *M2* made it more stable, increasing its convergence rate. Whereas, compared with *M1* variant, it failed to achieve the maximum possible fitness value. However, the inclusion of mutative randomization for enhancing the exploitation capability of the algorithm, helped in improving the convergence rate reducing premature convergence problem to an extent compared with the other counterparts. These studies gave scope for the inclusion of all three modifications to the standard CS algorithm, which in turn resulted in a more stable and reliable algorithm (ACSEA) as expected. Visual evaluation of these algorithms presented in Fig. 2 also proves that the proposed ACSEA yields the best brightness and contrast enhancement results with least image distortion and sharpness of

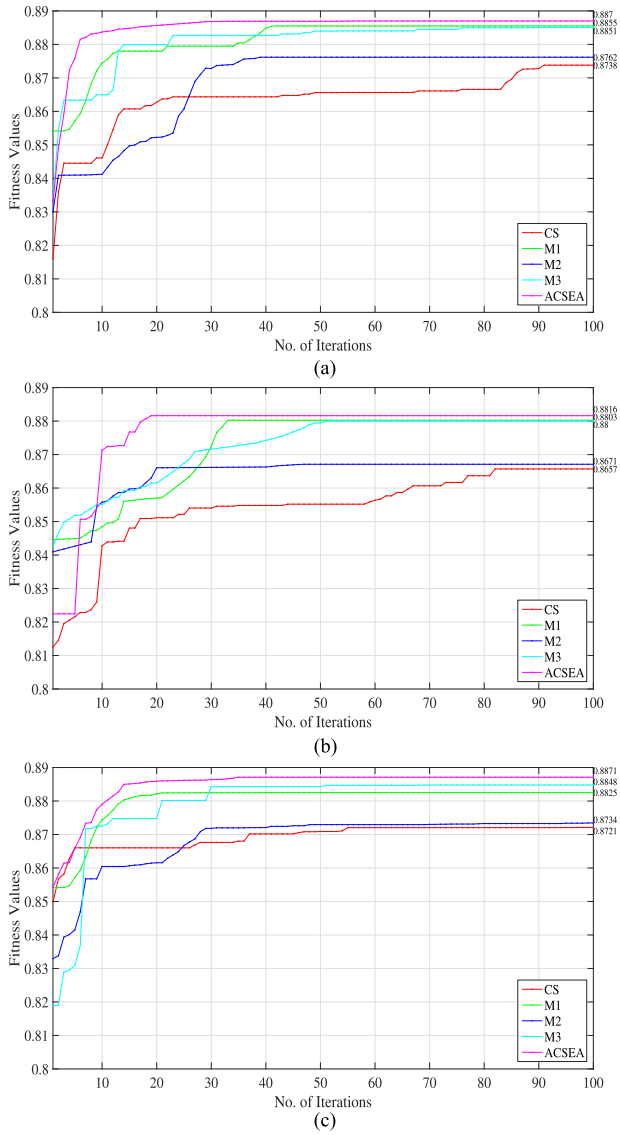

Fig. 3. Convergence analysis between modified versions of CS algorithm (a) R channel; (b) G channel; (c) B channel.

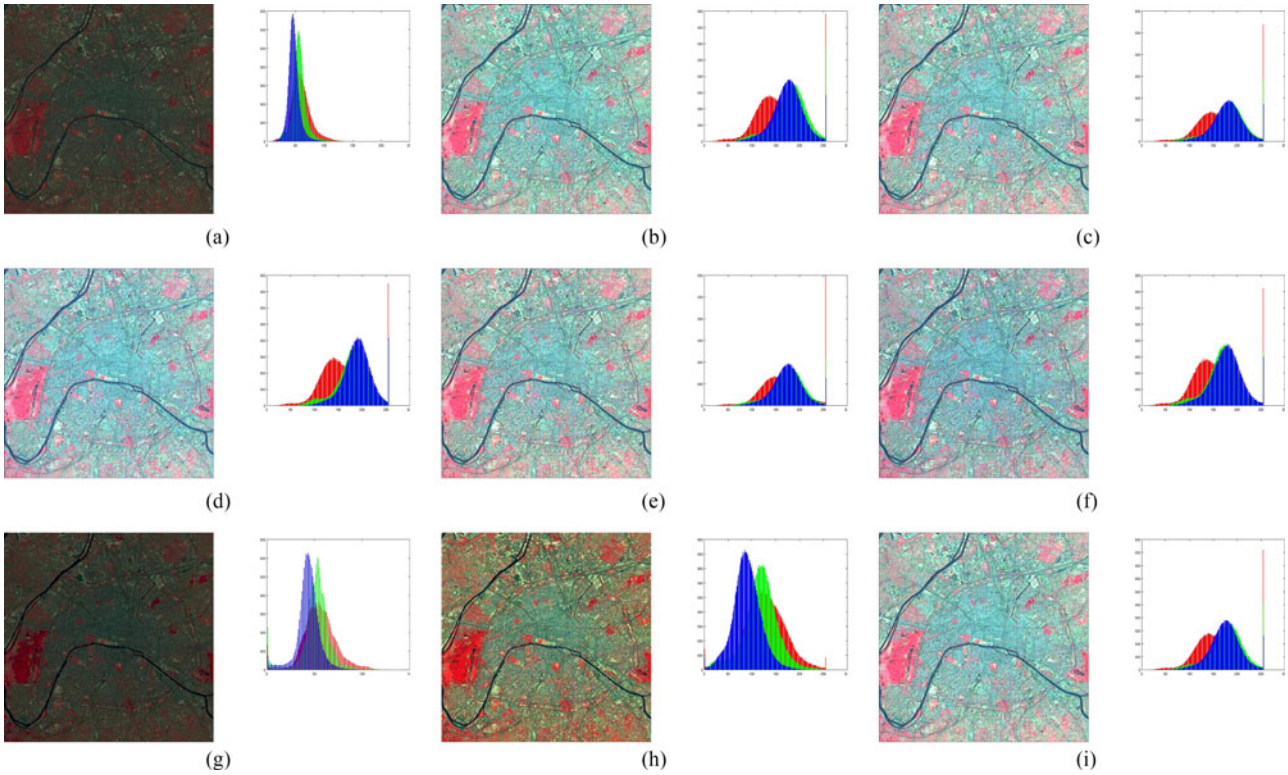

Fig. 4. Enhancement images and histograms of Image 1: Seine river, Paris, IKONOS data, (512 × 512, Multispectral, 50cm res., http://visibleearth.nasa.gov/) (a) Original; (b) A1; (c) A2; (d) A3; (e) A4; (f) A5; (g) A6; (h) A7; (i) ACSEA.

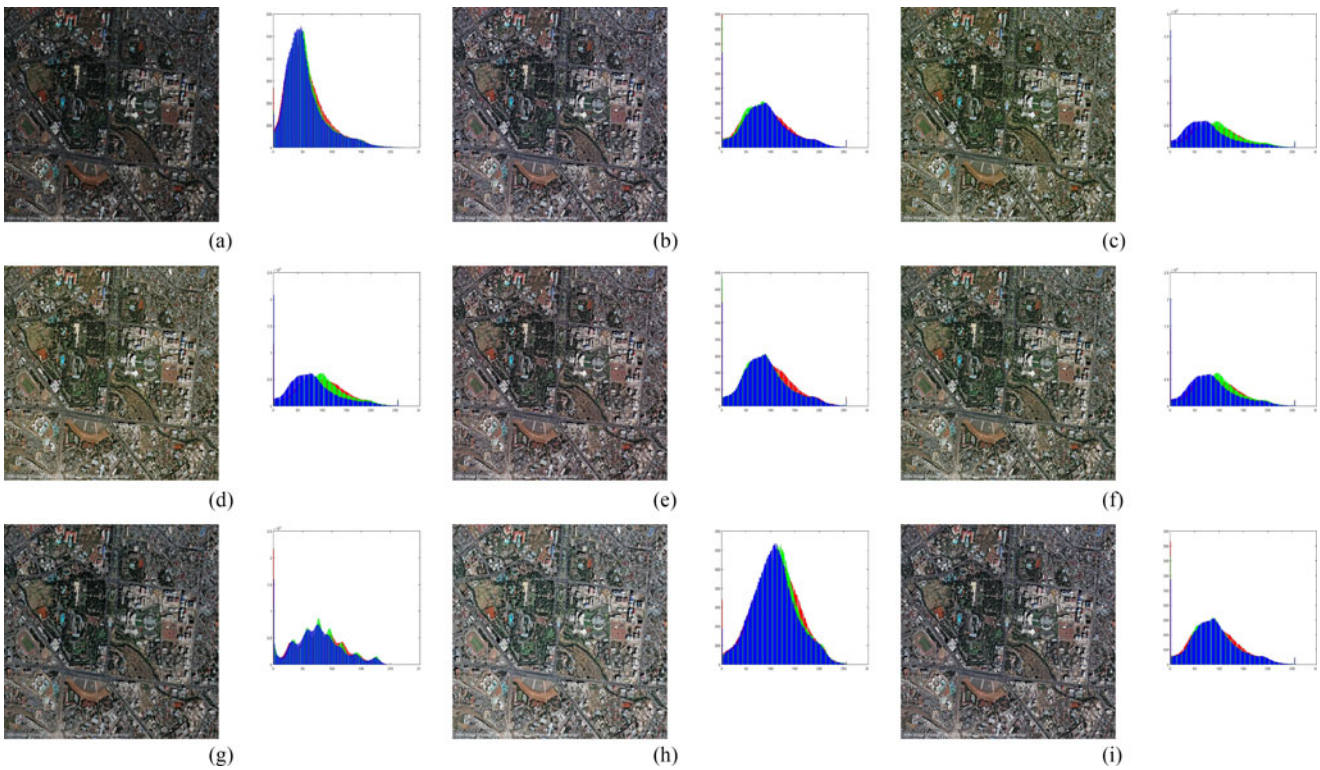

Fig. 5. Enhancement images and histograms of Image 2: Addis Ababa, Ethiopia (900 × 702, SPOT data, Multispectral, 50cm res. http://www.satimagingcorp.com/ gallery/) (a) Original; (b) A1; (c) A2; (d) A3; (e) A4; (f) A5; (g) A6; (h) A7; (i) ACSEA.

TABLE III
PERFORMANCE METRICS COMPARISON OF DIFFERENT ENHANCEMENT ALGORITHMS FOR IMAGE 1

Algorithm	PSNR	MSE	SSIM	CEF	UQI	SC-QI	SC-DM
A1	20.8161	538.849	0.6704	0.7318	0.9874	0.997	0.0026
A2	20.9177	526.3884	0.6666	0.7256	0.9859	0.9971	0.0025
A3	20.828	537.3828	0.6819	0.7323	0.9879	0.9971	0.0025
A4	20.8872	530.1087	0.6818	0.7546	0.9895	0.9971	0.0025
A5	20.2884	608.4762	0.6562	0.7326	0.983	0.9968	0.0027
A6	18.5028	917.9083	0.6236	0.9534	0.9035	0.9958	0.0042
A7	18.1747	989.9341	0.6328	0.7663	0.9261	0.9952	0.0046
ACSEA	**20.9239**	**525.6428**	**0.6889**	**0.9734**	**0.9976**	**0.9972**	**0.0021**

TABLE IV
PERFORMANCE METRICS COMPARISON OF DIFFERENT ENHANCEMENT ALGORITHMS FOR IMAGE 2

Algorithm	PSNR	MSE	SSIM	CEF	UQI	SC-QI	SC-DM
A1	22.6875	350.2127	0.8376	1.8507	0.9963	0.9994	0.0004
A2	23.5554	286.7741	0.8731	0.9716	0.9965	0.9988	0.0003
A3	22.8473	337.5581	0.858	0.9033	0.9976	0.999	0.0003
A4	23.3628	299.7767	0.8671	0.9892	0.9982	0.9997	0.0003
A5	21.6378	445.9641	0.8622	1.1236	0.9955	0.9997	0.0003
A6	20.8486	534.8314	0.8976	1.0076	0.9797	0.9978	0.0013
A7	21.9815	412.0332	0.8364	1.4443	0.9865	0.9991	0.0008
ACSEA	**23.6427**	**281.0697**	**0.8983**	**1.9291**	**0.9983**	**0.9998**	**0.0002**

features. The superior behavior of ACSEA is well supported by the computed metric values given in Table II.

Tables III and IV furnishes the results obtained on comparing the performance assessment measures discussed above for eight different enhancement algorithms given below. It clearly indicates that the proposed algorithm have a clear upper hand over the other seven algorithms.

PSNR value was observed to be comparatively higher for ACSEA, which quantifies the quality of the enhanced image. Low MSE and SCDM guarantees a minimum error/distortion for the processed image. Higher value for CEF ensures that ACSEA is efficient in preserving the mean intensity of the image thereby yielding naturalness to the scene. UQI and SCQI assessment indicates that ACSEA outperforms others in enhancing the local and global visual quality of the image being processed. SSIM metric that measures the amount of edge information of the processed image reveals that the proposed algorithm is very efficient in conserving the relevant edges and prominent features present in the original image making it adaptable for feature related processing tasks.

D. Visual Comparison

Figs. 4 and 5 give the subjective evaluation of enhanced images using all the eight enhancement algorithms compared. Comparison of histogram plots reveals that the proposed algorithm enhances the contrast of the input image by stretching the range of intensity values along its full range. The contrast stretching makes the minute details in the image more distinguishable for human interpretation. A close visual evaluation of processed images using ACSEA clearly indicates that every minor details in the input image is enhanced efficiently with

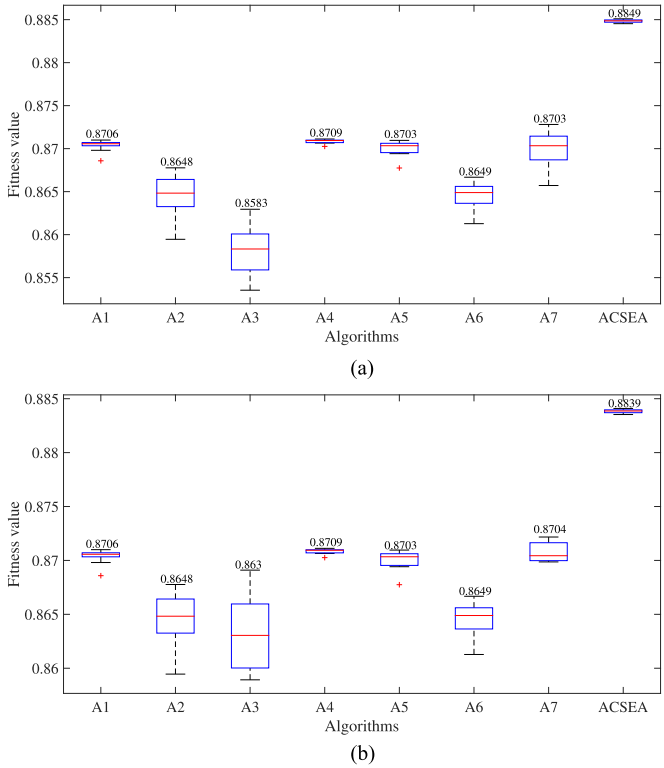

Fig. 6. Box plots of test images. (a) Image1; (b) Image2.

minimum artifacts. It also proved to be efficient in conserving the mean intensity of those images, thereby preserving its naturalness. The visual results also emphasizes the robustness of the proposed algorithm in enhancing different satellite image datasets.

E. Stability Analysis

Box-and -whisker plots shown in Fig. 6 evaluates the stability and converging capability of the compared algorithms to it global optimum solutions. It plots the final fitness values attained versus the algorithms used. The following box plots were obtained by executing each of the eight algorithms ten times for each of the test images included. Each run of the same algorithm for a particular image yielded a slightly different fitness solution and, hence, the optimum solution set. The stability of each algorithm is accounted by comparing the difference in the optimum fitness values obtained in a fixed number of runs. Smaller difference among the fitness values makes the algorithm more stable. The top and the bottom of the box are always chosen as the first and third quartiles. The variability of values outside those two quartiles are represented as vertical lines extending from the boxes (whiskers). The two ends of the whiskers in the given plots denotes the lowest datum, which is still included in the 1.5 interquartile range (IQR) of the lower quartile, and the highest datum included in 1.5 IQR of the upper quartile [61], [62]. The median value is shown above respective boxes and is indicated by a red line across each box in the plot.

Analyzing the plots, we can very well understand that the proposed ACSEA algorithm is most efficient in attaining the

maximum fitness score and, hence, converges to a global solution set. Stability analysis reveals that algorithms *A1*, *A4*, and ACSEA are the most stable among the set bringing least deviation in the final fitness values attained in consecutive runs. The plots also reveals the consistent stability of ACSEA for all the tested images emphasizing the robustness of the proposed algorithm. Among the eight different algorithms compared *A3* evolved as the least stable algorithm with a premature convergence. Ranking the compared algorithms in decreasing order of stability is given as ACSEA $> A4 > A1 > A5 > A6 > A7 \approx A2 > A3$. Ordering them according to their converging capability ranks them as ACSEA $> A4 > A1 > A7 > A5 > A2 > A6 > A3$.

V. Conclusion

In this paper, a novel ACSEA was proposed for contrast enhancement of satellite images. The enhancement process was automated by quantitatively optimizing the transformation function used for stretching the contrast curve. A chaotic initialization phase used by the proposed metaheuristic algorithm ensures a fast global convergence of the optimal solution set. The adaptive $L\acute{e}vy$ flight strategy helps in increasing the convergence rate of the algorithm. Whereas, the mutative randomization of the solution spaces balances the exploration and exploitation capability of the proposed algorithm.

Performance evaluation of the proposed enhancement algorithm was conducted by comparing it with state-of-the-art metaheuristic algorithms. Algorithms were tested on a wide range of satellite image datasets to measure its robustness. Visual comparison of the experimental results proved that the proposed ACSEA outperforms others in enhancing the contrast without compromising the naturalness of the scene. Quantitative evaluation gives substantial evidence to judge the proposed algorithm to be the most efficient among the set of compared enhancement algorithms for satellite image enhancement application.

The major merits of the proposed algorithm are: 1) it improved the convergence rate of the standard CS optimization algorithm by reducing the problem of premature convergence; and 2) the adaptive modifications increased its adaptability across different image datasets, ensuring the best possible results. But it badly suffers the limitation of being computationally a little complex in its execution. The proposed algorithm also leaves a scope for its applicability in the preprocessing stages of various image classifications.

Acknowledgment

The authors would like to thank the editors and anonymous reviewers for their valuable suggestions and comments which helped to improve the quality of the research paper.

References

[1] G. Cheng, J. Han, L. Guo, Z. Liu, S. Bu, and J. Ren, "Effective and efficient midlevel visual elements-oriented land-use classification using vhr remote sensing images," *IEEE Trans. Geosci. Remote Sensing*, vol. 53, no. 8, pp. 4238–4249, Aug. 2015.

[2] F. Zhang, B. Du, and L. Zhang, "Saliency-guided unsupervised feature learning for scene classification," *IEEE Trans. Geosci. Remote Sensing*, vol. 53, no. 4, pp. 2175–2184, Apr. 2015.

[3] X. Lu, Y. Wang, and Y. Yuan, "Graph-regularized low-rank representation for destriping of hyperspectral images," *IEEE Trans. Geosci. Remote Sens.*, vol. 51, no. 7, pp. 4009–4018, Jul. 2013.

[4] X. Lu and X. Li, "Multiresolution imaging," *IEEE Trans. Cybern.*, vol. 44, no. 1, pp. 149–160, Jan. 2014.

[5] S. M. Pizer *et al.*, "Adaptive histogram equalization and its variations," *Computer Vis., Graph., Image Process.*, vol. 39, no. 3, pp. 355–368, Sep. 1987.

[6] S. M. Pizer, R. E. Johnston, J. P. Ericksen, B. C. Yankaskas, and K. E. Muller, "Contrast-limited adaptive histogram equalization: Speed and effectiveness," in *Proc. IEEE 1st Conf. Visualization Biomed. Comput.*, May 1990, pp. 337–345.

[7] R. C. Gonzalez and R. E. Woods, *Digital image processing*. Englewood Cliffs, NJ, USA: Prentice-Hall, Oct. 2008.

[8] S. Hashemi, S. Kiani, N. Noroozi, and M. E. Moghaddam, "An image contrast enhancement method based on genetic algorithm," *Pattern Recognit. Lett.*, vol. 31, no. 13, pp. 1816–1824, Oct. 2010.

[9] E. Lee, S. Kim, W. Kang, D. Seo, and J. Paik, "Contrast enhancement using dominant brightness level analysis and adaptive intensity transformation for remote sensing images," *IEEE Geosci. Remote Sens. Lett.*, vol. 10, no. 1, pp. 62–66, Jan. 2013.

[10] H. Demirel, C. Ozcinar, and G. Anbarjafari, "Satellite image contrast enhancement using discrete wavelet transform and singular value decomposition," *IEEE Geosci. Remote Sens. Lett.*, vol. 7, no. 2, pp. 333–337, Apr. 2010.

[11] R. A. Schowengerdt, *Techniques for Image Processing and Classifications in Remote Sensing*. New York, NY, USA: Academic, Dec. 2012.

[12] A. Rosenfeld and A. C. Kak, *Digital picture processing*, vol. 1. Amsterdam, The Netherlands: Elsevier, Jan. 2014.

[13] L. Xie, G. Wang, X. Zhang, B. Xiao, B. Zhou, and F. Zhang, "Remote sensing image enhancement based on wavelet analysis and histogram specification," in *Proc. IEEE 3rd Int. Conf. Cloud Comput. Intell. Syst.*, Nov. 2014, pp. 55–59.

[14] X. Fu, J. Wang, D. Zeng, Y. Huang, and X. Ding, "Remote sensing image enhancement using regularized-histogram equalization and DCT," *IEEE Geosci. Remote Sens. Lett.*, vol. 12, no. 11, pp. 2301–2305, Nov. 2015.

[15] K. Huang, S. Li, X. Kang, and L. Fang, "Spectral–spatial hyperspectral image classification based on KNN," *Sens. Imag.*, vol. 17, no. 1, pp. 1–13, Dec. 2016.

[16] S. K. Pal, D. Bhandari, and M. K. Kundu, "Genetic algorithms for optimal image enhancement," *Pattern Recognit. Lett.*, vol. 15, no. 3, pp. 261–271, Mar. 1994.

[17] F. Saitoh, "Image contrast enhancement using genetic algorithm," in *Proc. IEEE Int. Conf. Syst., Man, Cybern.*, Jan. 1999, vol. 4, pp. 899–904.

[18] C. Munteanu and V. Lazarescu, "Evolutionary contrast stretching and detail enhancement of satellite images," in *Proc. Mendel*, 1999, pp. 94–99.

[19] C. Munteanu and A. Rosa, "Towards automatic image enhancement using genetic algorithms," in *Proc. IEEE Congr. Evol. Comput.*, Jul. 2000, vol. 2, pp. 1535–1542.

[20] M. Braik, A. F. Sheta, and A. Ayesh, "Image enhancement using particle swarm optimization," in *Proc. World Cong. Eng.*, Jul. 2007, vol. 1, pp. 978–988.

[21] A. Gorai and A. Ghosh, "Gray-level image enhancement by particle swarm optimization," in *Proc. IEEE World Cong. Nature Biol. Inspired Comput.*, Dec. 2009, pp. 72–77.

[22] A. Gorai and A. Ghosh, "Hue-preserving color image enhancement using particle swarm optimization," in *Proc. IEEE Recent Adv. Intell. Comput. Syst.*, Sep. 2011, pp. 563–568.

[23] L. dos Santos Coelho, J. G. Sauer, and M. Rudek, "Differential evolution optimization combined with chaotic sequences for image contrast enhancement," *Chaos, Solitons Fractals*, vol. 42, no. 1, pp. 522–529, Oct. 2009.

[24] N. M. Kwok, Q. P. Ha, D. Liu, and G. Fang, "Contrast enhancement and intensity preservation for gray-level images using multiobjective particle swarm optimization," *IEEE Trans. Autom. Sci. Eng.*, vol. 6, no. 1, pp. 145–155, Jan. 2009.

[25] P. Shanmugavadivu and K. Balasubramanian, "Particle swarm optimized multi-objective histogram equalization for image enhancement," *Opt. Laser Technol.*, vol. 57, pp. 243–251, Apr. 2014.

[26] A. Bhandari, A. Kumar, S. Chaudhary, and G. Singh, "A new beta differential evolution algorithm for edge preserved colored satellite image enhancement," *J. Multidimensional Syst. Signal Process.*, vol. 28, no. 2, pp. 495–527, Apr. 2017.
[27] V. Singh, G. Kumar, and G. Arora, "Analytical evaluation for the enhancement of satellite images using swarm intelligence techniques," in *Proc. IEEE 3rd Int. Conf. Comput. Sustainable Global Develop.*, Mar. 2016, pp. 2401–2405.
[28] C. Munteanu and A. Rosa, "Gray-scale image enhancement as an automatic process driven by evolution," *IEEE Trans. Syst., Man, Cybern. B, Cybern.*, vol. 34, no. 2, pp. 1292–1298, Apr. 2004.
[29] X. Zhou, Q. Shen, and J. Wang, "Research of image enhancement based on particle swarm optimization," *Microelectron. Comput.*, vol. 25, no. 4, pp. 42–44, May 2008.
[30] Z. Ye, M. Wang, Z. Hu, and W. Liu, "An adaptive image enhancement technique by combining cuckoo search and particle swarm optimization algorithm," *Comput. Intell. Neurosc.*, no. 13, pp. 1–12, Jan. 2015.
[31] R. Jain, R. Kasturi, and B. G. Schunck, *Machine vision*, vol. 5. New York, NY, USA: McGraw-Hill, Mar. 1995.
[32] J. Canny, "A computational approach to edge detection," *IEEE Trans. Pattern Anal. Mach. Intell.*, vol. PAMI-8, no. 6, pp. 679–698, Nov. 1986.
[33] P. L. Rosin, "Edges: Saliency measures and automatic thresholding," *Mach. Vis. Appl.*, vol. 9, no. 4, pp. 139–159, Feb. 1997.
[34] P. Sarangi, B. Mishra, B. Majhi, and S. Dehuri, "Gray-level image enhancement using differential evolution optimization algorithm," in *Proc. IEEE Int. Conf. Signal Process. Integr. Netw.*, Feb. 2014, pp. 95–100.
[35] A. K. Jain, *Fundamentals of Digital Image Processing*. Englewood Cliffs, NJ, USA: Prentice-Hall, Jan. 1989.
[36] X.-S. Yang and S. Deb, "Cuckoo search via Lévy flights," in *Proc. World Congr. Nature Biol. Inspired Comput.*, Dec. 2009, pp. 210–214.
[37] S. Suresh and S. Lal, "An efficient cuckoo search algorithm based multilevel thresholding for segmentation of satellite images using different objective functions," *Exp. Syst. Appl.*, vol. 58, pp. 184–209, Oct. 2016.
[38] H. Rakhshani and A. Rahati, "Snap-drift cuckoo search: A novel cuckoo search optimization algorithm," *Appl. Soft Comput.*, vol. 52, pp. 771–794, Mar. 2017.
[39] R. Caponetto, L. Fortuna, S. Fazzino, and M. G. Xibilia, "Chaotic sequences to improve the performance of evolutionary algorithms," *IEEE Trans. Evol. Comput.*, vol. 7, no. 3, pp. 289–304, Jun. 2003.
[40] L. Wang and Y. Zhong, "Cuckoo search algorithm with chaotic maps," *Math. Problems Eng.*, vol. 2015, Jul. 2015, Art. no. 715635.
[41] X.-S. Yang, *Nature-Inspired Optimization Algorithms*. Amsterdam, The Netherlands: Elsevier, Feb. 2014.
[42] M. Naik, M. R. Nath, A. Wunnava, S. Sahany, and R. Panda, "A new adaptive cuckoo search algorithm," in *Proc. Int. Conf. Recent Trends Inf. Syst.*, Jul. 2015, pp. 1–5.
[43] X. Li and M. Yin, "Modified cuckoo search algorithm with self adaptive parameter method," *Inform. Sci.*, vol. 298, pp. 80–97, Mar. 2015.
[44] J. Kennedy and R. Eberhart, "Particle swarm optimization," in *Proc. IEEE Int. Conf. Neural Netw.*, Piscataway, NJ, USA, May 1995, pp. 1942–48.
[45] R. Storn and K. Price, "Differential evolution—A simple and efficient heuristic for global optimization over continuous spaces," *J. Global Optim.*, vol. 11, no. 4, pp. 341–359, Dec. 1997.
[46] X.-S. Yang, "Firefly algorithm," in *Engineering Optimization*. Hoboken, NJ, USA: Wiley, Oct. 2010, pp. 221–230.
[47] Z. Bayraktar, M. Komurcu, and D. H. Werner, "Wind driven optimization (WDO): A novel nature-inspired optimization algorithm and its application to electromagnetics," in *Proc. IEEE Antennas Propag. Soc. Int. Symp.*, Jul. 2010, pp. 1–4.
[48] Z. Bayraktar, M. Komurcu, J. A. Bossard, and D. H. Werner, "The wind driven optimization technique and its application in electromagnetics," *IEEE Trans. Antennas Propag.*, vol. 61, no. 5, pp. 2745–2757, May 2013.
[49] A. Gogna and A. Tayal, "Metaheuristics: Review and application," *J. Exp. Theoretical Artif. Intell.*, vol. 25, no. 4, pp. 503–526, Dec. 2013.
[50] H. Ibrahim and N. S. P. Kong, "Brightness preserving dynamic histogram equalization for image contrast enhancement," *IEEE Trans. Consum. Electron.*, vol. 53, no. 4, pp. 1752–1758, Nov. 2007.
[51] H. Demirel, G. Anbarjafari, and M. N. S. Jahromi, "Image equalization based on singular value decomposition," in *Proc. 23rd Int. Symp. Comput. Inf. Sci.*, Oct. 2008, pp. 1–5.
[52] T. Hassanzadeh, H. Vojodi, and F. Mahmoudi, "Non-linear grayscale image enhancement based on firefly algorithm," in *Proc. Int. Conf. Swarm, Evol., Memetic Comput.*, Springer, Dec. 2011, pp. 174–181.
[53] S. Agrawal and R. Panda, "An efficient algorithm for gray level image enhancement using cuckoo search," in *Proc. Int. Conf. Swarm, Evol., Memetic Comput.*, Springer, Dec. 2012, pp. 82–89.
[54] A. Bhandari, V. Soni, A. Kumar, and G. Singh, "Cuckoo search algorithm based satellite image contrast and brightness enhancement using DWT–SVD," *ISA Trans.*, vol. 53, no. 4, pp. 1286–1296, Feb. 2014.
[55] J. Mukherjee and S. K. Mitra, "Enhancement of color images by scaling the DCT coefficients," *IEEE Trans. Image Process.*, vol. 17, no. 10, pp. 1783–1794, Oct. 2008.
[56] S. E. Susstrunk and S. Winkler, "Color image quality on the internet," *Proc. SPIE*, vol. 5304, pp. 118–131, Dec. 2003.
[57] Z. Wang, A. C. Bovik, H. R. Sheikh, and E. P. Simoncelli, "Image quality assessment: From error visibility to structural similarity," *IEEE Trans. Image Process.*, vol. 13, no. 4, pp. 600–612, Apr. 2004.
[58] Z. Wang and A. C. Bovik, "A universal image quality index," *IEEE Signal Process. Lett.*, vol. 9, no. 3, pp. 81–84, Mar. 2002.
[59] S.-H. Bae and M. Kim, "A novel image quality assessment with globally and locally consilient visual quality perception," *IEEE Trans. Image Process.*, vol. 25, no. 5, pp. 2392–2406, May 2016.
[60] S.-H. Bae and M. Kim, "A novel DCT-based JND model for luminance adaptation effect in DCT frequency," *IEEE Signal Process. Lett.*, vol. 20, no. 9, pp. 893–896, Sep. 2013.
[61] R. McGill, J. W. Tukey, and W. A. Larsen, "Variations of box plots," *Amer. Statistician*, vol. 32, no. 1, pp. 12–16, Feb. 1978.
[62] M. Frigge, D. C. Hoaglin, and B. Iglewicz, "Some implementations of the boxplot," *Amer. Statistician*, vol. 43, no. 1, pp. 50–54, Feb. 1989.

Shilpa Suresh (S'17) received the M.E. degree in communication systems from Hindustan University, Chennai, India, in 2012 and is currently working toward the Ph.D. degree in satellite image processing from National Institute of Technology, Karnataka, India.

Her research interest focuses on satellite image processing using stochastic metaheuristic algorithms.

Shyam Lal (M'11) received the M.Tech. degree in electronics and communication engineering from NIT kurukshetra, Kurukshetra, India, in 2007, and the Ph.D. degree in image processing from BIT Mesra, Ranchi, India, in 2013.

He has been working as an Assistant Professor in the Department of Electronics & Communication Engineering, National Institute of Technology Karnataka, Mangalore, India. His research interests include digital image processing, remote sensing, and medical image processing.

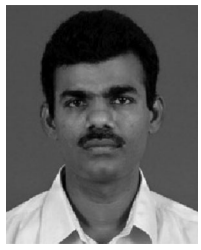

Chintala Sudhakar Reddy received the M.Sc. degree in botany from Osmania University, Hyderabad, India, in 1996, and the Ph.D. degree in botany from Kakatiya University, Warangal, India, in 2002.

In 2001, he joined the National Remote Sensing Centre, Indian Space Research Organization as a Scientist. He is currently working in the field of remote sensing and GIS applications in forestry and ecology. His current research interests include long-term forest cover change assessment for south Asian countries and biodiversity characterization.

Mustafa Servet Kiran received the M.Sc. and Ph.D. degrees in computer engineering from the School of Natural and Applied Sciences, Selcuk University, Konya, Turkey, in 2010 and 2014, respectively.

He is currently an Associate Professor in Computer Engineering Department, Selcuk University. His current research interests include evolutionary computation, neural computing, nature-inspired computation, and their applications.